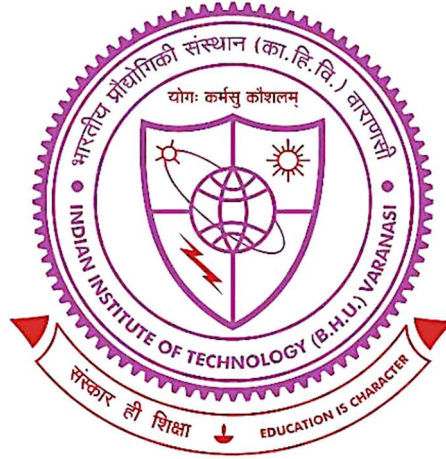


**Microstructural evolution and phase stability in binary
NiMn, semi-Heusler NiMnSb and NiMnSbV multicomponent
alloy**



**Thesis submitted in partial fulfilment for the
Award of Degree**

Doctor of Philosophy

By

Aman Kumar Lal Das

**DEPARTMENT OF METALLURGICAL ENGINEERING
INDIAN INSTITUTE OF TECHNOLOGY
(BANARAS HINDU UNIVERSITY)
VARANASI – 221005
INDIA**

Roll No. 16141001

2024

CERTIFICATE

It is certified that the work contained in the thesis titled “**Microstructural evolution and phase stability in binary NiMn, semi-Heusler NiMnSb and V added NiMnSb multicomponent alloy**” by “**Aman Kumar Lal Das**” has been carried out under my supervision and that this work has not been submitted elsewhere for a degree.

It is further certified that the student has fulfilled all the requirements of Comprehensive, Candidacy and SOTA for the award of Ph.D. degree.



Prof. Joysurya Basu

(Supervisor)

Associate Professor

Department of Metallurgical Engineering

Indian Institute of Technology

(Banaras Hindu University)

Varanasi

DECLARATION BY THE CANDIDATE

I, **Aman Kumar Lal Das**, certify that the work embodied in this Ph.D. thesis is my own bonafide work carried out under the supervision of **Prof. Joysurya Basu** for a period from **July 2016** to **June 2023** at the “**Department of Metallurgical Engineering**”, Indian Institute of Technology (BHU), Varanasi, India. The matter embodied in this Ph.D. thesis has not been submitted for the award of any other degree/diploma. I declare that I have faithfully acknowledged and given credits to the research workers wherever their works have been cited in my work in this thesis. I further declare that I have not willfully copied any other's work, paragraphs, text, data, results, etc., reported in journals, books, magazines, reports dissertations, thesis, etc., or available at websites and have not included them in this thesis and have not cited as my own work.

Date : July 22, 2024

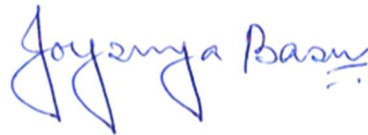
Place : Varanasi

Aman Kumar Lal Das

(Aman Kumar Lal Das)


CERTIFICATE BY THE SUPERVISOR

This is to certify that the above statement made by the candidate is correct to the best of my knowledge.



Prof. Joysurya Basu
(Supervisor)
Department of Metallurgical Engineering
Indian Institute of Technology (Banaras Hindu University)
Varanasi

Forwarded by:



(Head of the Department)
Department of Metallurgical Engineering
Indian Institute of Technology
(Banaras Hindu University)
Varanasi – 221005, India

COPYRIGHT TRANSFER CERTIFICATE

Title of the Thesis: Microstructural evolution and phase stability in binary NiMn, semi-Heusler NiMnSb and NiMnSbV multicomponent alloy.

Candidate's Name: Aman Kumar Lal Das

COPYRIGHT TRANSFER

The undersigned hereby assigns to the Indian Institute of Technology (Banaras Hindu University), Varanasi all rights under copyright that may exist in and for the above thesis submitted for the award of the *Doctor of Philosophy*.

Date: July 22, 2024

Place: Varanasi

Aman Kumar Lal Das

(Aman Kumar Lal Das)

Note: However, the author may reproduce or authorize others to reproduce materials extracted verbatim from the thesis or derivative of the thesis for author's personal use provided that the source and the Institute's copyright notice are indicated.

Acknowledgement

I want to inaugurate my acknowledgement statement by offering my gratitude to the almighty God for the wisdom he has showered over me that has made my path easy to this attainment.

I am expressing my sincere gratitude to my supervisor Prof. Joysurya Basu, for imparting his knowledge and expertise in this work. I am very fortunate to have learnt the fundamentals of materials characterization techniques and crystallography from him. He has not only trained me on transmission electron microscopy but also introduced me with related advanced characterization techniques, such as in-situ TEM, EELS, HAADF-STEM-XEDS, etc. In combination with hands on experience, he has also made me familiar with essential analytical tools such as multislice image simulation (JEMS), crystal structure identification (Rietveld refinement) and other analytical software. His emphasis over squeezing the gathered data at the fullest, has implanted a sense of critical thinking and developed the ability of thinking out of the box. He has always advised me to prefer quality over quantity, which immensely benefited me in publishing my research work in reputed journals. In simple words, his amiable and enthusiastic nature and clear vision has helped me greatly in uplifting my understanding of such an intricate subject. I am extremely thankful to him for his untiring support throughout my Ph.D. journey, specially the push he gave me every time I have got stuck. It is my pleasure working under his guidance.

It is my privilege to express my heartfelt gratitude to him for giving me the latitude to perform various experiments irrespective of their success probability, which has immensely helped me in developing concept out of the book. His innovative approach towards research, always enhances my propensity toward research and inspired me to remain positive and be patient in all ups and downs. He is a thorough observer and a patient researcher, he listens to my all queries and tries to turn them into a logical discussions that always boosts up my confidence. His approach of putting the intricate things in simple and elusive manner has always inspired me to attain perfection in my work. I am indebted to him for inspiring guidance, persistent encouragement throughout the course of this work.

I would also like to convey my thanks to Profs. R.K.Mandal and N. K. Mukhopadhyay, for fruitful discussions and, former Heads of the Department for their kind support. I

thank Prof. Sunil Mohan, the current Head of the Department for his valuable contribution.

I also want to show respect to the all faculty members of Department of Metallurgical Engineering, IIT (BHU) for creating such a wonderful environment for research. I would also like to express my gratitude to the entire non-teaching staff of the Metallurgical Engineering Department of IIT BHU.

It is my pleasure to thank Prof. Rajiv Kumar Mandal, Department of Metallurgical Engg, IIT (BHU), Prof. Rajesh Prasad, Department of Materials Science and Engg. IIT Delhi for involving in frequent and long discussion sessions, which has helped me improving my knowledge of crystallography to take my work up to next level and I am also grateful to MIT opencourseware for providing the lectures of Prof. Berhardt Wuensch, Department of Materials Engg. MIT Cambridge on symmetry and tensors. I gratefully acknowledge Prof. Ashok Mondal, Metallurgical Engineering, IIT(BHU), for giving me financial support from his DST project which I very much needed in that tough period. Working with all of them have been a great learning experience.

I am grateful to my present and former labmates, Prof. Manish Singh, Dr. Vikas Shivam, Prof. Raj Bahadur, Dr. Vivek Pandey, Prof. Yagnesh Shadangi, Prof. Rajkumar Deshwar, Dr. Asnit Gangwar, Dr. Ankit Singh, Dr. Subham Shaw, Vinay, Sankata, Roopchand, Saarika, Soham, Satyam, Purnendu and Gaurav, for their cheerful company. I also want to convey my thanks to Lalit Da and Dr. Avnish Singh Pal for their unconditional support and readiness for any kind of help.

At personal front, I wish to express my sincere gratitude and indebtedness to my family for their blessings, care, encouragement and moral support throughout this journey.

Aman Kumar Lal Das
(Aman Kumar Lal Das)

Table of contents

Abbreviations.....	
Symbols.....	
Preface.....	
1. Chapter 1	1
1.1 “Allotropic” and “Polymorphic” transformation.....	1
1.2 Quasi-chemical theory for the formation of solid solution or intermetallic	10
1.3 Miedema’s Model	11
1.4 Intermetallics.....	12
1.4.1 Stoichiometric intermetallic compounds	12
1.4.2 Non-stoichiometric intermetallic compounds.....	13
1.4.3 Electron compounds / Hume-Rothery compounds.....	13
1.4.4 Frank-Kasper phases / Size factor compounds.....	14
1.4.4.1 A-15 compounds.....	14
1.4.4.2 Laves Phase.....	14
1.4.4.3 σ , μ , M, P, and R phases	14
1.4.5 Heusler Alloys.....	15
1.5 High-entropy alloys.....	16
1.6 Alloy Design Strategies.....	20
1.6.1 Strength-Ductility Trade off Dilemma	21
1.6.2 Inverse Hall-Petch Relationship.....	22
1.6.3 Structure-Property Correlations	23
1.6.4 Grain Boundary Engineering.....	24
1.7 High-energy Ball Milling	25
1.7.1 Extension of solid solubility.....	25
1.7.2 Refinement of grain size to nanoscale range.....	26
1.7.3 Formation of intermetallic, metastable phases and quasicrystal.....	26
1.8 Motivation and Objectives	28
2. Chapter 2.....	29
2.1 Materials and alloy synthesis.....	29
2.1.1 Vacuum Induction Melting.....	30
2.1.2 Differential Scanning Calorimetry.....	30
2.1.2 High energy ball milling.....	31
2.2 Crystal Structure and microstructural characterization.....	32
2.2.1 X-ray diffraction.....	32
2.2.2 Scanning electron microscopy.....	32
2.2.3 Transmission electron microscopy.....	33

3.	Chapter 3.....	35
	3.1 Introduction.....	35
	3.2 Experimental Techniques.....	36
	3.3 Results	37
	3.4 Discussion.....	40
	3.5 Conclusions.....	48
4.	Chapter 4.....	49
	4.1 Introduction.....	49
	4.2 Experimental Techniques.....	50
	4.3 Results.....	52
	4.4 Discussion.....	61
	4.4.1 Phase formation and stability.....	61
	4.4.2 Microstructural evolution.....	66
	4.4.3 Structure and defects in NiMnSb and NiMnSbV.....	67
	4.5 Conclusions.....	69
5	Chapter 5.....	71
	5.1 Introduction.....	71
	5.2 Experimental Techniques.....	73
	5.3 Results.....	74
	5.4 Discussion.....	82
	5.4.1 Processing route dependence of phase evolution.....	82
	5.4.2 Effect of configurational entropy.....	84
	5.4.3 Role of atomic size and enthalpy of mixing.....	85
	5.5 Conclusions.....	86
6	Chapter 6	89
	6.1 Conclusions.....	89
	6.2 Suggestions for future work.....	90
	References	93-113

List of Publications

List of Conference Presentations

List of Tables

Table 1.1	Different phases showing stability with their respective composition range along with the crystallographic information in Ni-Sb equilibrium phase diagram	6
Table 1.2	Different phases showing stability with their respective composition range along with the crystallographic information in Mn-Sb equilibrium phase diagram	8
Table 1.3	Different phases showing stability with their respective composition range alongwith the crystallographic information in Ni-Mn equilibrium phase diagram	9
Table 1.4	Classification of electron compounds on basis of their electron-atom ratio	13
Table 2.1	Physical properties of the elements for the synthesis of alloys	29
Table 2.2	Protocol for mechanical alloying of powders	31
Table 3.1	Calculation of structure factor for different planes for Structure I and Structure II	43
Table 4.1	Relative difference in atomic radii (in %) between Ni, Mn, Sb and V	63
Table 4.2	Binary Enthalpy of mixing at infinite dilution between Ni, Mn, Sb and V (kJ/mol)	63

List of Figures

Figure 1.1	Gibbs free energy - Temperature plot at constant pressure (a) showing the condition of allotropism or polymorphism prior to melting (b) showing the condition of melting prior to allotropism or polymorphism	3
Figure 1.2	The hierarchy of symmetries and the phase transformation route among the seven crystal systems	4
Figure 1.3	Equilibrium Phase Diagram of Ni-Sb	5
Figure 1.4	Equilibrium Phase Diagram of Mn-Sb	7
Figure 1.5	Equilibrium Phase Diagram of Ni-Mn	9
Figure 3.1	(a) Experimental x-ray diffraction pattern of the as solidified NiMn alloy (b) simulated x-ray diffraction pattern of tI2 NiMn (red) and cF4 NiMn phase (cyan) (c) simulated x-ray diffraction pattern of tI2 NiMn (red) and mP8 NiMn (cyan) phase. Both the simulated patterns show a good match with the experimental pattern.	38
Figure 3.2	(a) TEM bright field image of the as solidified NiMn alloy in which alternative bright and dark contrast leading to a chessboard like pattern is observed. (b-d) experimental electron diffraction pattern from the bright domains along $z=[131]$, $[111]$ and $[113]$ zone axes of tI2 NiMn phase, (e-h) simulated electron diffraction patterns from the tI2 NiMn phase along $z= [131]$, $[111]$, $[113]$ and $[110]$ zone axes. The simulated patterns are in scale with the experimental patterns in (b-d). (i-l) experimental electron diffraction patterns from the dark domains of the as solidified NiMn alloy. The experimental patterns show superlattice reflections along $[110]$ and $[112]$ directions, when compared to the simulated patterns of tI2 NiMn phase.	39
Figure 3.3	(a) Schematic representation of the disordered tetragonal lattice in which Ni and Mn atoms are shown in some of the lattice positions by average atoms. (b) schematic representation of the same tetragonal lattice in which order has been introduced along $[110]$ direction resulting into the doubling of the lattice spacing along $[110]$ with respect to the tI2 NiMn phase. (c) schematic representation of (001) plane in which order has been introduced along $[010]$ and $[110]$ (d) schematic representation of the (001) plane in which order has been introduced along $[100]$ and $[010]$ (e) Schematic representation of Structure I, which is obtained by stacking Layer A on Layer A with a relative displacement of $\frac{1}{4}[110]$ (f) schematic representation of Structure II, which is obtained by stacking Layer B on Layer A with $\frac{1}{4}[110]$ relative displacement.	41

Figure 3.4	(a-d) Experimentally observed electron diffraction patterns and (e-h) corresponding simulated electron diffraction patterns from the new mP8 NiMn phase in the as solidified alloy.	44
Figure 3.5	Simulated electron diffraction pattern of mP8 phase from [110] zone axis showing unallowed reflections circled in white	45
Figure 3.6	(a) HAADF image of the as solidified NiMn alloy in which alternating bright and dark contrast arising out of the two related phases can be observed. (b-c) XEDS spectral map on Ni and Mn respectively, in which no composition segregation is observed. (d) streaks in the ordered phase mP8 can be observed. (e) tweed structures in the ordered mP8 phase with different variants can be observed. (f) coherent interface at the disordered tI2 and mP8 phase can be observed.	46
Figure 3.7	DSC thermogram of equi-atomic NiMn system showing various solid state phase transformations at 523 °C, 705 °C, 802 °C in correlation with the phase diagram.	47
Figure 4.1	XRD pattern of induction melted and as solidified (a) NiMnSb semi-Heusler alloy, which shows only standard FCC reflections (b) NiMnSbV alloy, which shows additional SbV ₃ reflections (marked in blue) along with the standard reflections from the semi-Heusler NiMnSb phase. (c) Rietveld refined pattern ($\chi^2 = 1.7914$) of (a) which confirms the presence of FCC semi-Heusler NiMnSb phase only (d) Rietveld refined pattern ($\chi^2 = 1.4231$) of (b) which confirms the presence of cubic SbV ₃ phase along with the cubic semi-Heusler NiMnSb phase.	52
Figure 4.2	(a) SEM micrograph (b) XEDS spectra of induction melted and as solidified NiMnSb alloy. In the SEM micrograph solidification shrinkage porosities are observed and in the XEDS spectra almost equi-atomic distribution of Ni, Mn and Sb is observed. (c) SEM micrograph (d) XEDS spectra of the SbV ₃ phase in the induction melted and as solidified NiMnSbV alloy. In the SEM micrograph, along with solidification shrinkage porosities, semi-Heusler NiMnSb and cubic SbV ₃ phases are observed. Lamellar structures at the interface of two phases are present. The SbV ₃ phase is almost stoichiometric as confirmed from the XEDS spectra in (d).	54
Figure 4.3	(a-b): Visible light micrograph of induction melted and as solidified NiMnSbV alloy in which mildly faceted islands of SbV ₃ phase in the matrix of semi-Heusler NiMnSb phase is observed. Lamellar structure is quite often observed at the interface of the two phases.	55
Figure 4.4	Multiple display of in-situ XRD patterns of induction melted and as solidified (a) NiMnSb, (b) NiMnSbV alloy recorded at room temperature (RT), 200, 400, 600 and 700 °C. In both the alloys, from 400 °C, hexagonal (Ni/Mn)Sb phase evolves at the expense of the cubic semi-Heusler NiMnSb parent phase while	56

- the cubic SbV_3 phase appears to be stable in the temperature range of investigation.
- Figure 4.5 (a,c) TEM bright field images (b,d) corresponding rotationally oriented electron diffraction patterns from the induction melted and as solidified NiMnSb semi-Heusler alloy. In the bright field images of the semi-Heusler phase, bend contours and dislocations are observed. Electron diffraction patterns along $Z=[100]$ in (c) and $Z=[111]$ in (d) confirms the cubic structure of the semi-Heusler phase 58
- Figure 4.6 (a, c) TEM bright field images and (b,d) corresponding rotationally oriented electron diffraction patterns from the SbV_3 phase in the induction melted and as solidified NiMnSbV alloy. In the bright field image in (a), linear contrast is observed due to the layered structure of the compound and due to the presence of defects in the phase. The corresponding electron diffraction pattern in (b) along $Z=[212]$ shows that the phase is cubic and the presence of the superlattice reflections (marked with red arrows) confirms that the phase repeats in every fourth layer. In the bright field image in (c), linear contrast typical of twins can be observed and it is confirmed through the electron diffraction pattern in (d), in which 200 is the unique row of reflections signifying that the twin planes are $\{200\}$ type. 59
- Figure 4.7 (a) in-situ TEM bright field image of NiMnSbV as-solidified alloy captured at 400°C , where the nucleation of (Ni/Mn)Sb phase can clearly be seen in NiMnSb phase which is oriented along $[100]$ and (b) the interface of NiMnSb and SbV_3 , where SbV_3 does not show any phase transformation. 60
- Figure 4.8 Change in enthalpy (ΔH) vs. composition plots for binaries (a) Ni-Mn (b) Ni-Sb (c) Mn-Sb (d) Ni-V (e) Mn-V (f) Sb-V as calculated by Miedema's model. ΔH solid solution (ΔH^{sol}), ΔH amorphous (ΔH^{am}), ΔH elastic (ΔH^{e}) and ΔH chemical (ΔH^{c}) are plotted in green, blue, red and black respectively for all the binary systems. 64
- Figure 4.9 Polyhedral diagram for cubic SbV_3 phase. (a) Edge sharing 12-fold coordination icosahedra with Sb atom at the center (b) 14-fold coordination polyhedra with V atom at the center. 68
- Figure 5.1 (a) Multiple display of x-ray diffraction patterns of mechanically alloyed Ni, Mn, Sb powders after 10 h, 40 h, 70 h and 100 h (b) Multiple display of x-ray diffraction patterns of mechanically alloyed Ni, Mn, Sb, V after 10 h, 40 h, 70 h and 100 h. 75
- Figure 5.2 (a) Multiple display of x-ray diffraction patterns of mechanically alloyed Ni, Mn, Sb powder after milling for 10 h, 40 h, 70 h and 100 h. (b) Simulated x-ray diffraction pattern of newly formed disordered hexagonal phase showing a good match with the experimental pattern. 76

- Figure 5.3 The graphs represent the variation of crystallite size, crystallite strain and volume fraction of the newly phase formed against the mechanical alloying duration. 77
- Figure 5.4 (a-d) The SEM micrographs of mechanically alloyed powders of NiMnSb and (e-h) NiMnSbV at different alloying duration 78
- Figure 5.5 (a-f): TEM bright field images and corresponding electron diffraction patterns from different regions of the NiMnSb alloy after milling for 100 h. (a-b) Disordered hexagonal solid solution phase with high dislocation density and the corresponding electron diffraction pattern along $z=[101]$. (c-d) Nanoparticles of disordered hexagonal solid solution phase embedded in the amorphous matrix and the corresponding electron diffraction pattern showing randomly oriented crystals. (e-f) Amorphous phase in the alloy with corresponding electron diffraction pattern represented by the diffused halo. 79
- Figure 5.6 (a-d): TEM bright field images and corresponding electron diffraction patterns from different regions of the NiMnSbV alloy after milling for 100 h. (a) Cluster of faceted crystals of disordered hexagonal phase of NiMnSbV. (b) corresponding nano-beam electron diffraction pattern from one particle in (a) showing explicit 6-fold rotational symmetry from $z=[001]/[0001]$ of the disordered hexagonal solid solution phase. (c) showing the presence of the amorphous phase with some embedded nanocrystals (d) corresponding electron diffraction pattern showing the amorphous phase as represented by the diffused halo and the disordered hexagonal phase as represented by the presence of the discontinuous Debye rings. 81
- Figure 5.7 (a) The highest intensity (101) peak of (Ni/Mn)Sb showing the intensity profile for NiMnSb mechanically alloyed powders after 10 h and 40 h of alloying respectively (b) The highest intensity (101) peak of (Ni/Mn)Sb showing the intensity profile for NiMnSbV mechanically alloyed powders after 10 h, 40 h and 70 h of alloying respectively. 85

Abbreviations

HEA	:	High Entropy Alloy
CCA	:	Complex Concentrated Alloy
MPEA	:	Multi Principal Elemental Alloy
BMG	:	Bulk Metallic Glass
SPSS	:	Single Phase Solid Solution
HEBM	:	High Energy Ball Milling
STEM	:	Scanning Transmission Electron Microscope
CSL	:	Coincidence Site Lattice
GBE	:	Grain Boundary Engineering
MA	:	Mechanical Alloying
BF	:	Bright Field
DF	:	Dark Field
XEDS	:	X-ray Energy Dispersive Spectroscopy
NBED	:	Nano Beam Electron Diffraction
XRD	:	X-ray Diffraction
TEM	:	Transmission Electron Microscope
SG	:	Space Group
FCC	:	Face Centred Cubic
BCC	:	Body Centred Cubic
HCP	:	Hexagonal Close Packed

Symbols

θ	:	Bragg angle
λ	:	Wavelength
ΔH	:	Enthalpy of formation
ε	:	Misfit strain
ΔG	:	Free energy
d	:	Interplanar spacing
a	:	Lattice parameter
$^{\circ}$:	Degree
ϵ	:	Strain
c	:	Elastic constant
δ	:	Small fraction